Universität Stuttgart

Copyright Notice

Generalized 8-PSK for Totally Blind Channel Estimation in OFDM

Marc C. Necker

Institute of Communication Networks and Computer Engineering,
University of Stuttgart
Pfaffenwaldring 47, D-70569 Stuttgart, Germany
Email: necker@ikr.uni-stuttgart.de
Tel.: +49 711 685 7963   Fax: +49711 685 7983

Frieder Sanzi[1]

Business Unit Logistics
Leuze Electronic GmbH + Co KG
In der Braike 1, D-73277 Owen/Teck, Germany
Email: friedrich.sanzi@leuze.de
Tel.: +49 7021 573 323   Fax: +49 7021 573 199

Abstract— **Channel estimation in OFDM systems can conveniently be done by inserting a stream of pilot symbols at the transmitter and by using FIR interpolation filters at the receiver. The drawback of this method is the decrease in spectral efficiency due to the pilot symbols. Alternatively, blind channel estimation makes pilot symbols unnecessary. Most blind channel estimation approaches are based on higher order statistics and converge slowly, making them unsuitable for mobile environments. Moreover, the channel estimate suffers from a phase blindness, which can only be resolved by pilot symbols. The concept of totally blind channel estimation makes pilots completely unnecessary and even works in rapidly time varying environments. This is achieved by using two different modulation schemes, such as QPSK and 3-PSK, on adjacent subcarriers. In this paper, we further develop the concept of totally blind channel estimation by applying a regular 8-PSK and a generalized 8-PSK to achieve totally blind channel estimation without the need for any pilot symbols. We enhance the original receiver design by applying a two-dimensional A Posteriori Probability (APP) calculation algorithm. We evaluate our system at high Doppler frequencies with COST 207 channels on the basis of Extrinsic Information Transfer (EXIT) and BER charts.**

I. INTRODUCTION

Orthogonal Frequency Division Multiplex (OFDM) has become very popular since it is well suitable for multipath-fading environments. If coherent demodulation is desired, the receiver needs to know the time-variant channel transfer function (CTF). The CTF can conveniently be estimated using a two-dimensional grid of pilot symbols [1]. However, the overhead introduced by pilot symbols might be quite significant. Digital Video Broadcasting – Terrestrial [2] is one such example, where the overhead from pilots is more than 10%.

The amount of pilot symbols can greatly be reduced by applying the APP (A Posteriori Probability) based channel estimation (CE) method presented in [3]. Two one-dimensional APP estimators in frequency and time direction, respectively, are concatenated in order to obtain an estimate of the two-dimensional CTF. To improve the estimation results, the APP estimators can be embedded in an iterative decoding loop.

The APP-method according to [3] still needs some pilot symbols. In contrast, blind channel estimation algorithms are supposed to estimate the CTF without the help of pilot symbols. Most research in the field of blind channel estimation has focused on methods which are based on second or higher

order statistics. Examples include those algorithms using correlation methods [4] and cumulant fitting schemes [5]. Other blind algorithms for OFDM take advantage of the redundancy introduced by the guard interval [6]. Most of these approaches converge slowly, making them unsuitable for mobile environments. Moreover, they can recover the CTF only with a phase ambiguity. To recover the phase information completely, additional reference symbols need to be inserted into the data stream. Even though only a few reference symbols are needed, the charm of blind channel estimation is lost.

In [7], a fast converging blind channel estimator based on the Maximum Likelihood principle was introduced. The phase ambiguity was resolved without the help of any reference symbols by using QPSK and 3-PSK on adjacent subcarriers. Since absolutely no pilots or training sequences are needed, this approach is called *Totally Blind Channel Estimation*, in contrast to other blind channel estimation algorithms which cannot recover the complete phase information without pilots.

In this paper, we enhance the totally blind approach of [7] by the APP algorithm. We further extend our studies to the combination of 8-PSK and 7-PSK, as well as 8-PSK and generalized 8-PSK in order to resolve the phase ambiguity.

This paper is organized as follows: In section II, the transmitter, receiver and channel model are detailed. Section III introduces the concept of totally blind channel estimation and the used modulation schemes. The APP channel estimation approach is described in section IV. Finally, section V presents selected simulation results.

II. SYSTEM MODEL

A. Transmitter and receiver

We investigate an OFDM-system with $K = 1000$ subcarriers having a carrier-spacing of $\Delta f = 4\,\mathrm{kHz}$. The signal from the binary source is convolutionally encoded and interleaved as shown in Fig. 1. After interleaving, three successive coded bits are mapped onto an 8-ary symbol $X_{k,l}$. The signal $X_{k,l}$ is modulated onto K orthogonal sub-carriers by an iFFT-block. Finally, a cyclic prefix of length 1/4 is inserted.

The channel's output signal is corrupted by AWGN. After removal of the cyclic prefix and OFDM demodulation we obtain the received 8-ary signal constellation points $Y_{k,l}$:

$$Y_{k,l} = H_{k,l} \cdot X_{k,l} + N_{k,l}, \tag{1}$$

where l is the OFDM symbol index, k is the sub-carrier index and $N_{k,l}$ are statistically i.i.d. complex Gaussian noise
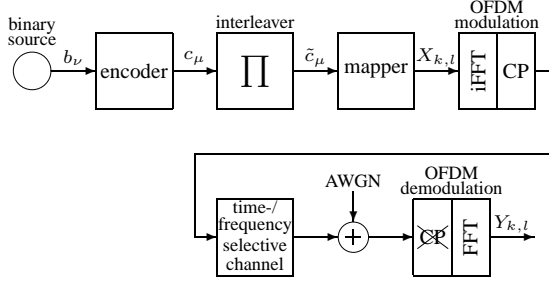
Fig. 1: Transmitter, channel model and OFDM demodulation.

variables. The $H_{k,l}$ are sample values of the CTF:

$$H_{k,l} = H(k \cdot \Delta f, l \cdot T_{\mathrm{s}}) \ , \tag{2}$$

where T_{s} is the OFDM-symbol duration. The signal $Y_{k,l}$ is fed to the blind APP-CE stage as shown in Fig. 2. This stage outputs log-likelihood ratios (L-values) on the transmitted coded bits which are deinterleaved and decoded in an APP decoder. Iterative channel estimation and decoding is performed by feeding back extrinsic information on the coded bits; after interleaving it becomes the *a-priori* knowledge to the blind APP-CE stage.

We use a recursive systematic convolutional code with feedback polynomial $G_{\mathrm{r}} = 037_8$, feed-forward polynomial $G = 023_8$, memory 4 and code rate $R_{\mathrm{c}} = 0.5$. Note that in the following all E_{b}/N_0-values are given with respect to the overall information rate $R = R_{\mathrm{c}} \cdot R_{\mathrm{g}} = 0.4$, whereby R_{g} considers the redundancy introduced by the cyclic prefix:

$$R_{\mathrm{g}} = \frac{1}{\Delta f \cdot T_{\mathrm{s}}} = 0.8 \tag{3}$$

B. Channel model

For the performance evaluation we assumed a frequency-selective fading channel according to a wide-sense stationary uncorrelated scattering (WSSUS) model. The channel was simulated according to the model introduced in [8], which describes the channel's time-variant impulse response as

$$h(\tau, t) = \lim_{Z \to \infty} \frac{1}{\sqrt{Z}} \sum_{m=1}^{Z} e^{j\theta_m} e^{j2\pi f_{\mathrm{D}max} t} \delta(\tau - \tau_{max}) \ . \tag{4}$$
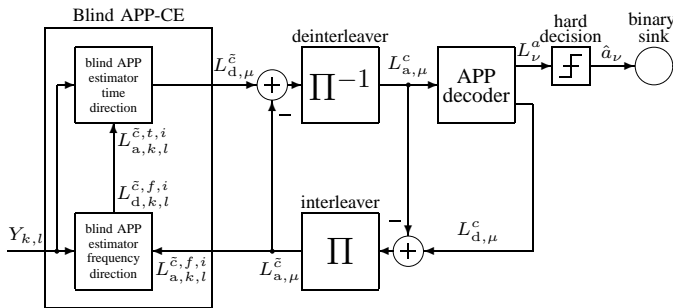

Fig. 2: Receiver with iterative blind APP channel estimation.

The Fourier-Transform of equation (4) with respect to τ yields the channel's time-variant frequency response:

$$H(f, t) = \lim_{Z \to \infty} \frac{1}{\sqrt{Z}} \sum_{m=1}^{Z} e^{j\theta_m} e^{j2\pi f_{\mathrm{D}max} t} e^{-j2\pi f \tau_{max}} \ . \tag{5}$$

For each of the Z paths, the phase-shift θ_m, the Doppler-shift $f_{\mathrm{D}max}$ and the delay τ_m are randomly chosen from the corresponding probability density function (pdf) $p_\theta(\theta)$, $p_{f_{\mathrm{D}}}(f_{\mathrm{D}})$ or $p_\tau(\tau)$ of the channel model [8]. For the simulations, the number of paths was set to $Z = 100$. The channel models were chosen according to the well known models in COST 207 [9].

III. TOTALLY BLIND CHANNEL ESTIMATION

In [10], the authors present a blind channel estimation approach based on the ML-principle, which essentially exploits the finite alphabet property of the transmitted data symbols. It works solely in the frequency-direction on just one OFDM-symbol. As a consequence, we will restrict our derivations to the frequency direction. However, we applied the same concepts in the time direction as well.

Consider a vector $\mathbf{y}$ of M data symbols received on adjacent subcarriers and a vector $\mathbf{x}$ with the corresponding M transmitted data symbols. If $\mathbf{X}$ is a diagonal matrix with the transmitted symbols as diagonal elements, and $\mathbf{h}$ is a vector with the corresponding and unknown M channel transfer function coefficients in the frequency domain, the following minimum equation needs to be solved [10]:

$$\hat{\Psi} = \min_{\Psi} \|\mathbf{y} - \mathbf{Xh}\|^2 \quad , \quad \Psi := [\mathbf{h}^T, \mathbf{x}^T]^T \ . \tag{6}$$

In the general case, at least $M_{\min}$ subcarriers need to be considered in order to be able to uniquely solve equation (6). $M_{\min}$ was derived in [10] and depends on the channel's delay spread, the subcarrier-spacing and the modulation scheme. For channels with long delay spreads or for higher order modulation schemes, $M_{\min}$ is very large, which makes equation (6) extremely complex to solve.

Consider two adjacent subcarriers with indices $k = 0$ and $k = 1$. In [7] it was shown that as few as $M = 2$ received symbols on adjacent subcarriers are sufficient to uniquely determine the CTF on these subcarriers. This is possible if the CTF does not vary too fast in frequency direction, that is $h_0 \approx h_1$. Under the assumption that $h_1 \approx h_0 = y_0 x_0^*$ in the PSK-case, (6) reduces to

$$\begin{aligned}
\hat{\Psi} &= \min_{\Psi} \|\mathbf{y} - \mathbf{Xh}\|^2 \\
&= \min_{\Psi} \left(\|y_0 - h_0 x_0\|^2 + \|y_1 - h_1 x_1\|^2 \right) \\
&\approx \min_{\Psi} \left(\|y_0 - y_0 \underbrace{x_0^* x_0}_{=1}\|^2 + \|y_1 - y_0 x_0^* x_1\|^2 \right) \\
&= \min_{\Psi} \|y_1 - y_0 x_0^* x_1\|^2 = \min_{\Psi} \|y_1 - y_0 e^{j(\varphi_1 - \varphi_0)}\|^2 \\
&= \min_{\Psi} \|y_1 - y_0 e^{j\alpha}\|^2 \ , \tag{7}
\end{aligned}$$

with * denoting the complex conjugate, $x_0 = e^{j\varphi_0}$ and $x_1 = e^{j\varphi_1}$ in the PSK-case. Obviously, the angle $\alpha = \varphi_0 - \varphi_1$ is the only parameter that can be varied in order to

solve the minimum equation. This introduces the well-known phase ambiguity if only one modulation scheme is used. The ambiguity can be resolved by using two different modulation schemes on the two adjacent subcarriers. Theorem 2 in [7] states that if q_i is a signal point of the first PSK-modulation scheme, and q_j a signal point of the second PSK-modulation scheme, the signal points must be chosen such that no two angles $\alpha_{i,j} = \angle(q_i, q_j)$ are identical for all possible signal point combinations i, j. For example, QPSK and 3-PSK fulfill this condition, but also 8-PSK and 7-PSK [7]. In these cases, (7) can be solved without any ambiguity.

The condition of an approximately constant CTF for adjacent subcarriers holds for channels with a small delay spread, but does not hold anymore for channels with a longer delay spread. This imposed problems to the algorithm presented in [7] in combination with channels with a relatively long delay spread.

Theorem 3 from [7] stated that it is possible to consider not only two, but an arbitrary number of subcarriers M at a time in order to solve equation (6). By taking more subcarriers into account, the effect of noise can be mitigated. However, the complexity of the problem increases exponentially with M.

Following from [3], APP-CE is a trellis-based approach to solve eq. (6) in the presence of noise with respect to an appropriately chosen metric (see also section IV). In contrast to the algorithm in [7], where only a small number of subcarriers could be considered at a time, the trellis-based APP approach allows us to consider the complete OFDM-symbol at a time. Hence, the APP-CE needs only very little *a-priori* information to perform the channel estimation. In the pilot-based case, this *a-priori* information is obtained from the pilot symbols. In contrast to that, the *a-priori* information comes from the uniqueness of the angle α in our scheme.

This concept, which was just derived for the frequency direction, can also be applied in the time direction. Depending on the Doppler shift, the CTF remains approximately constant from one OFDM-symbol to the other. Hence, the two-dimensional APP-estimator can take advantage of the CTF correlation in both the frequency and the time direction. In all of our simulations, the two-dimensional estimator operated on blocks of 100 OFDM-symbols.

In this paper, we study the combination of 8-PSK and 7-PSK. We also investigate the possibility of combining 8-PSK with a generalized 8-PSK modulation scheme with signal points $\mathcal{S}_i^8$ according to (compare Fig. 3):

$$\mathcal{S}_i^8 = e^{ji\frac{2\pi}{\eta}} \;, 0 \le i \le 7, \, \eta \in \mathbb{R} \; . \tag{8}$$

$\eta = 7$ corresponds to a 7-PSK. In this case, the signal point at e^{j0} is occupied twice, which corresponds to a puncturing of the convolutional code, similar to the 3-PSK-mapping in [7]. Depending on η, the condition that no two angles $\alpha_{i,j}$ may be identical (see above) may or may not be fulfilled.

The following mapping from the coded bits to the signal points was used:

$\{000_2 \rightarrow \mathcal{S}_0^8, \; 100_2 \rightarrow \mathcal{S}_1^8, \; 101_2 \rightarrow \mathcal{S}_2^8, \; 111_2 \rightarrow \mathcal{S}_3^8, \\ 110_2 \rightarrow \mathcal{S}_4^8, \; 010_2 \rightarrow \mathcal{S}_5^8, \; 011_2 \rightarrow \mathcal{S}_6^8, \; 001_2 \rightarrow \mathcal{S}_7^8\}$
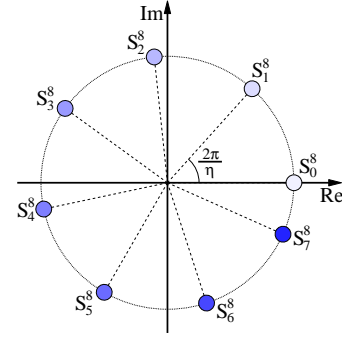

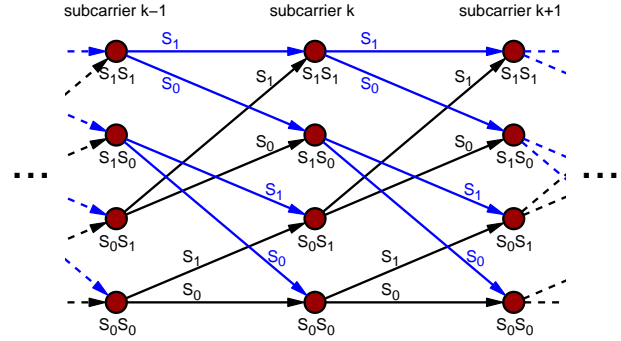Fig. 3: Generalized 8-PSK modulation scheme

Fig. 4: Artificial Trellis for BPSK

IV. APP CHANNEL ESTIMATION

As detailed in [3], the two-dimensional APP channel estimator consists of one estimator for frequency and time direction, respectively. Each of these one-dimensional estimators exploits the continuity of the CTF in either the frequency or the time direction by building up an artificial trellis of the data symbols. By doing so, it essentially searches for the most likely transmitted symbol sequence based on an appropriately chosen metric. Since the derivation of the algorithm in frequency and time direction is similar, we will restrict ourselves to the derivation in frequency direction.

Consider the transmitter's output symbol sequence in the frequency domain $X_{k,l}$. If we imagine these symbols being fed into a virtual shift register, we can build up an artificial trellis. This is illustrated in Fig. 4 for a shift register of length 2 and a BPSK modulation scheme with the two signal points S_0 and S_1.

On the receiver side, the CTF needs to be taken into account for each state transition. In our case, a linear predictor is used to predict the CTF for each state in the trellis. This prediction is based on the previously visited states, since an assumption of the transmitted data symbols has to be made:

$$\hat{H}_{k,l_0}^f = \sum_{i=1}^{m_f} u_{f,i} \cdot \frac{Y_{k-i,l_0}}{\hat{X}_{k-i,l_0}}. \tag{9}$$

If the statistical properties of the channel are known, the FIR filter coefficients $u_{f,i}$ can be calculated with the Wiener-Hopf equation based on the channel's auto-correlation. In [11], two such methods were derived and compared. In the
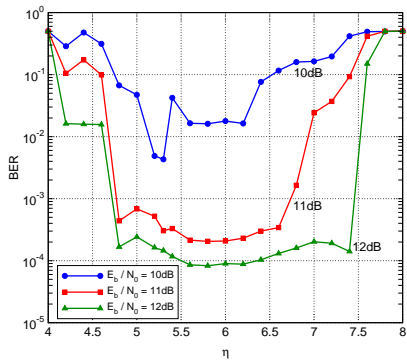
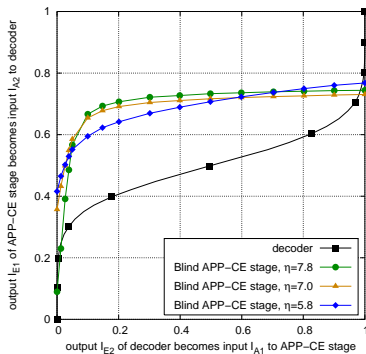Fig. 5: BER charts for COST 207 channel TU and different E_b/N_0 values. $f_{d_{max}} = 300\,\text{Hz}$

Fig. 6: EXIT chart for COST 207 channel TU and different values of η. $E_b/N_0 = 10\,\text{dB}$, $f_{d_{max}} = 300\,\text{Hz}$
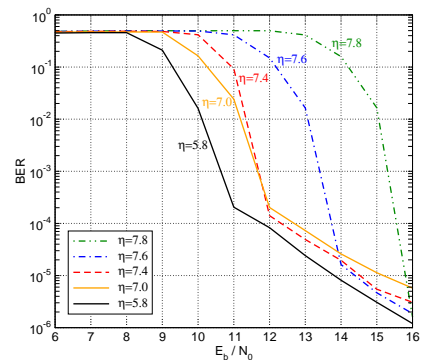

Fig. 7: BER charts for channel TU and different values of η. $f_{d_{max}} = 300\,\text{Hz}$
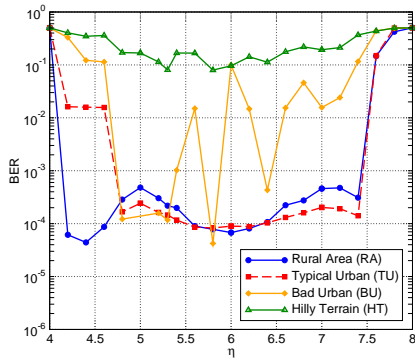

Fig. 8: BER over η for different channel models, $E_b/N_0 = 12\,\text{dB}$, $f_{d_{max}} = 300\,\text{Hz}$
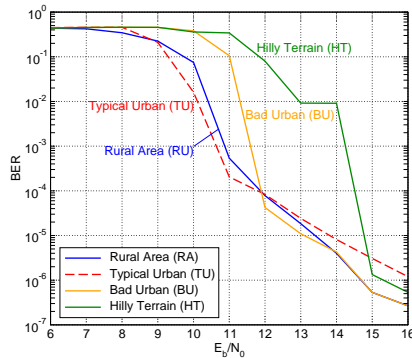

Fig. 9: BER charts for different channel models. $\eta = 5.8$, $f_{d_{max}} = 300\,\text{Hz}$

following, we will assume that the receiver has no knowledge of the channel at all. Consequently, the FIR filter coefficients cannot be calculated with the Wiener-Hopf equation. Instead, a generic set of predictor coefficients has to be used. In [11], the generic set $u_{f,i} = 1/m_f$ was discussed. Following from [11], we choose a filter order of $m_f = 1$ with $u_{f,i=0} = 1$ and $u_{f,i\neq0} = 0$. For all our simulations, we used this set of predictor coefficients in both the frequency and time direction.

V. SIMULATION RESULTS

All BER results in this section were measured after 4 iterations of the iterative decoding loop. This is sufficient to achieve maximum performance in all considered cases.

We first investigate the influence of the parameter η of the generalized 8-PSK modulation scheme. Fig. 5 shows the BER for a COST 207 Typical Urban (TU) channel at a high maximum Doppler frequency of $f_{D_{max}} = 300\,\text{Hz}$ for values of η between 4 and 8. The corresponding EXIT-chart for selected values of η is depicted in Fig. 6. Both charts show that the original idea from [7] of applying a 7-PSK ($\eta = 7$) is feasible. However, it can clearly be stated that this is not the optimal value. Instead, from Fig. 5 it follows, that $\eta = 5.8$ (i.e., a "5.8-PSK" modulation scheme) delivers the optimal performance for the underlying scenario. Note that the system cannot perform for $\eta = 8$ and $\eta = 4$, since Theorem 2 from [7] is not fulfilled. However, it is interesting to notice that

$\eta = 6$ delivers excellent BER performance, even though the same theorem is not fulfilled (note that some signal points of the 6-PSK are occupied twice). The reason for this is that Theorem 2 from [7] is fulfilled for a large enough number of adjacent subcarriers, but not all of them[1]. As the APP estimator needs only very little *a-priori* information, decoding of the data stream is still possible.

For the same scenario, Fig. 7 plots the BER results over E_b/N_0 for selected values of η. This chart emphasizes that even a very small deviation of 0.2 from the regular 8-PSK ($\eta = 7.8$) is sufficient in order to be able to decode the received data stream, although only at a high E_b/N_0. In accordance with Fig. 5, it is possible to decode the received data stream at lower values of E_b/N_0 if the deviation from the regular 8-PSK becomes larger.

So far, we restricted our evaluation to the very popular channel Typical Urban (TU). In the following, we will extend our analysis to the other channel models defined in COST 207 [9], namely Rural Area (RU), Bad Urban (BU) and Hilly Terrain (HT). With a maximum delay spread of almost $20\mu s$, HT is the worst considered channel profile.

Fig. 8 and Fig. 9 show the BER for the four channel models

---

[1] Note that due to the application of error correction codes all signal points are equally probable. Therefore, it is very unlikely that Theorem 2 is not fulfilled on a sufficient amount of adjacent subcarriers.
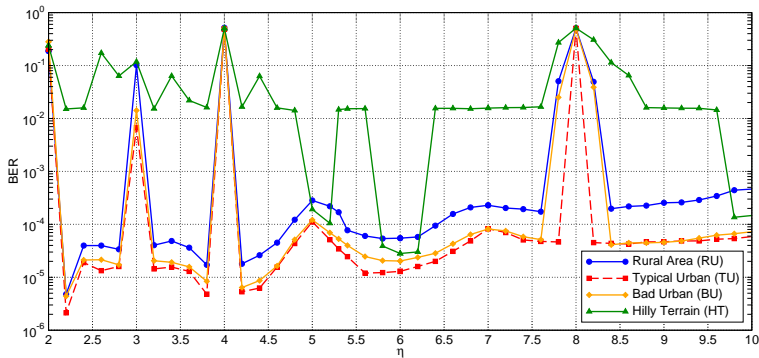
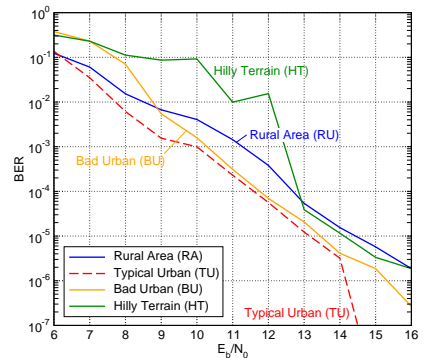Fig. 10: BER over η for different COST 207 channel models, $E_b/N_0 = 12\,\text{dB}$, $f_{d_{max}} = 100\,\text{Hz}$

Fig. 11: BER charts for different channel models. $\eta = 5.8$, $f_{d_{max}} = 100\,\text{Hz}$

over η and over E_b/N_0, respectively. The maximum Doppler shift was set to $f_{d_{max}} = 300\,\text{Hz}$. At such a high Doppler frequency, the channel HT cannot be handled at a reasonable E_b/N_0 anymore. The reason for this is the fast varying CTF in frequency and time direction (cmp. section III), which would make a better set of prediction coefficients necessary [11]. Whereas channels RA and TU expectedly impose no problems at all, channel BU with a maximum delay spread of 10μs is more difficult to handle. However, with $\eta = 5.8$, a competitive performance can be achieved at a target BER of 10^{-4}. Note that $\eta = 6$ delivers bad performance since Theorem 2 from [7] is not fulfilled, in contrast to channels RA and TU.

It is interesting to note that the BER performance of channel RA is slightly worse compared to that of channel TU for $E_b/N_0 < 12\,\text{dB}$. In this case the slow variation of the CTF for channel RU is a disadvantage, since the channel might be in a fade for a large block of subcarriers, which is not the case with channel TU. This leads to bad estimation results and block errors for these subcarriers.

Finally, we will consider the case of a smaller maximum Doppler shift, which results in a slower variation of the CTF in time direction. As a consequence, the APP estimator in time direction will perform better, which can make up for a bad performance of the APP estimator in frequency direction with channels with a long delay spread.

Fig. 10 and Fig. 11 show the BER for the four channel models over η and over E_b/N_0, respectively, with $f_{d_{max}} = 100\,\text{Hz}$. From Fig. 10 we can see that it is now possible to handle all channel profiles, even the profile HT. However, it becomes obvious that the proper selection of η is crucial. Again, $\eta = 5.8$ is a good choice for all channel models. The BER chart in Fig. 11 shows that a BER of 10^{-4} can be achieved with all channels at a reasonable E_b/N_0.

VI. CONCLUSION

We enhanced the totally blind channel estimation algorithm from [7] by the APP method. Additionally, the originally used QPSK and 3-PSK modulation scheme was replaced by a regular 8-PSK and a generalized 8-PSK modulation scheme in which the angle η between the signal points was varied. A value of $\eta = 5.8$ was found to give optimum performance in the considered scenarios. The system was investigated in a rapidly time-varying environment in combination with the channel models proposed in COST 207. It was shown that all COST 207 channels can be handled at a maximum Doppler shift of $f_{d_{max}} = 100\,\text{Hz}$. Despite the channel HT, all other COST 207 channels delivered good BER performance even at $f_{d_{max}} = 300\,\text{Hz}$. This was achieved with a very simple set of prediction coefficients, and we expect to be able to handle even channel HT with a more sophisticated predictor. Our simulations show that blind channel estimation with a non-adaptive receiver is possible with higher order modulation schemes and most realistic channels. The channel transfer function can thereby completely be recovered with no phase ambiguity without even a single reference symbol.

REFERENCES

[1] P. Höher, S. Kaiser, and P. Robertson, "Two–dimensional pilot–symbol–aided channel estimation by Wiener filtering," in *Proc. IEEE ICASSP*, Munich, Germany, April, 1997, pp. 1845–1848.

[2] "Digital video broadcasting (DVB); framing structure, channel coding and modulation for digital terrestrial television (DVB-T)," *European Telecommunication Standard, ETS 300744*, March 1997.

[3] F. Sanzi and S. ten Brink, "Iterative channel estimation and decoding with product codes in multicarrier systems," in *IEEE Vehicular Technology Conference*, Boston, USA, September, 2000, pp. 1338–1344.

[4] B. Muquet and M. de Courville, "Blind and semi-blind channel identification methods using second order statistics for OFDM systems," in *Proc. IEEE ICASSP*, Phoenix, AZ, USA, March, 1999, pp. 2745–2748.

[5] S. Chen, Y. Wu, and S. McLaughlin, "Genetic algorithm optimization for blind channel identification with higher order cumulant fitting," *IEEE Trans. on Evolutionary Computation*, vol. 1, no. 4, pp. 259–265, November, 1997.

[6] U. Tureli and H. Liu, "Blind carrier synchronization and channel identification for OFDM communications," in *Proc. IEEE ICASSP*, Seattle, WA, USA, May, 1998, pp. 3509–3512.

[7] M. C. Necker and G. L. Stüber, "Totally blind channel estimation for OFDM over fast varying mobile channels," in *Proc. IEEE International Conf. on Communications*, New York, USA, April, 2002, pp. 421–425.

[8] P. Höher, "A statistical discrete-time model for the WSSUS multipath channel," *IEEE Trans. on Vehicular Technology*, vol. 41, no. 4, pp. 461–468, November, 1992.

[9] COST 207 WG1, "Proposal on channel transfer functions to be used in GSM tests late 1986," *CEPT*, September 1986.

[10] N. Chotikakamthorn and H. Suzuki, "On identifiability of OFDM blind channel estimation," in *Proc. Vehicular Technology Conference 1999 - Fall*, Amsterdam, The Netherlands, September 1999, pp. 2358–2361.

[11] M. C. Necker and F. Sanzi, "Impact of linear prediction coefficients on totally blind APP channel estimation," in *Proc. 5th International ITG Conference on Source and Channel Coding (SCC)*, Erlangen, Germany, January 2004, pp. 317–324.